TSINGHUA SCIENCE AND TECHNOLOGY
ISSN 1007-0214 06/24 pp1341–1354
DOI: 10.26599/TST.2023.9010125
Volume 29, Number 5, October 2024

Distributed Robust UAVs Formation Control Based on Semidefinite Programming

Peiyu Zhang, Jianshan Zhou*, Daxin Tian, Xuting Duan, Dezong Zhao, and Kan Guo

Abstract: The formation control of unmanned aerial vehicle (UAV) swarms is of significant importance in various fields such as transportation, emergency management, and environmental monitoring. However, the complex dynamics, nonlinearity, uncertainty, and interaction among agents make it a challenging problem. In this paper, we propose a distributed robust control strategy that uses only local information of UAVs to improve the stability and robustness of the formation system in uncertain environments. We establish a nominal control strategy based on position relations and a semi-definite programming model to obtain control gains. Additionally, we propose a robust control strategy under the rotation set Ω to address the noise and disturbance in the system, ensuring that even when the rotation angles of the UAVs change, they still form a stable formation. Finally, we extend the proposed strategy to a quadrotor UAV system with high-order kinematic models and conduct simulation experiments to validate its effectiveness in resisting uncertain disturbances and achieving formation control.

Key words: multi-unmanned aerial vehicle (UAV) systems; formation control; uncertain perturbation; robust distributed control

1 Introduction

Over recent decades, formation control of unmanned aerial vehicle (UAV) swarms has drawn considerable attention in various domains such as transportation[1–3], emergency management[4–6], environmental monitoring[7, 8], and military defense[9, 10]. For instance, Yinka-Banjo and Ajayi[11] discussed different types of UAVs and their use in crop irrigation, health monitoring, animal mustering, geo-fencing, and other agricultural activities, showcasing their potential in advancing sustainable farming practices. Outay et al.[12] pointed out that drones have played a significant role in accident investigation and damage assessment pertaining to bridges and sidewalks. Furthermore, they are expected to utilize computer vision integration algorithms to extract crucial information from videos and images captured by drones, which will subsequently contribute to risk assessment processes. According to Ref. [13], major industry players like Amazon have been employing drones for package delivery since 2013.

With the increasing complexity and variability of deployment tasks, the significance of the UAVs control problem has become increasingly prominent[14]. Among these, fixed-wing UAVs stand out due to their long endurance and long-distance communication capabilities, giving them a clear advantage in task execution. Consequently, numerous scholars have

• Peiyu Zhang, Jianshan Zhou, Daxin Tian, Xuting Duan, and Kan Guo are with School of Transportation Science and Engineering, Beihang University, Beijing 100191, China. E-mail: zpeiyu2@163.com; jianshanzhou@foxmail.com; dtian@buaa.edu.cn; duanxuting@buaa.edu.cn; guokan.cn@gmail.com.
• Dezong Zhao is with James Watt School of Engineering, University of Glasgow, Glasgow, G12 8QQ, UK. E-mail: dezong.zhao@glasgow.ac.uk.
* To whom correspondence should be addressed.
Manuscript received: 2023-07-04; revised: 2023-09-15; accepted: 2023-10-16

conducted extensive research on the control of fixed-wing UAVs. Dierks and Jagannathan[15] introduced a novel nonlinear controller for a quadrotor UAV utilizing neural networks (NNs) and output feedback. The proposed approach incorporates an NN to learn the complete dynamics of the UAV in real time. Li et al.[16] proposed a UAV speed control framework based fairness data collection scheme to enhance data collection fairness in intelligent transportation systems. Paw and Balas[17] introduced an integrated framework for the development of small UAV flight control which offers a systematic procedure for designing flight control, accompanied by a suite of design tools that enable control engineers to efficiently synthesize, analyze, and validate controller designs. However, fixed-wing UAVs are extremely vulnerable to uncertain disturbances in the external environment when performing tasks (flights), so we will focus on the problem of UAV swarm formation control in uncertain environments.

The intricate dynamics, nonlinearity, uncertainties, and interactions between agents present substantial challenges in realizing effective formation control for UAVs[18]. To address this challenge, a wide array of control strategies have been proposed, predominantly encompassing centralized control and distributed control paradigms. Cao et al.[19] introduced a novel approach to control a swarm of fixed-wing UAVs, enabling them to maintain a parallel formation of a specific geometry. This scalable method utilizes decentralized cooperative control laws that ensure global stability. It considers the nonholonomic dynamics of the UAVs and input constraints, allowing for flexible initial positions. Li et al.[20] investigated the cooperative control problem in feedforward nonlinear time-delay multiagent systems. In this system, a static low-gain observer is proposed for each following UAV, and a distributed output feedback controller with a static gain is designed to achieve consensus. Bayezit and Fidan[21] presented a distributed control scheme for decentralized cohesive motion control of autonomous vehicles or robot formations in three dimensions. The scheme ensures that a formation can still be formed when damage occurs to one UAV. In Ref. [22], a behaviour-based algorithm has been proposed for UAV formation. Zhang et al.[23] proposed a UAV system control theory based on the backstepping method to enable the UAVs to form a stable formation quickly. In addition, Slotine and Sastry[24] designed a sliding mode controller to improve UAV vibration. Wu et al.[25] proposed a tracking control method for a high-order UAV system by integrating adjacent UAV information with consensus theory.

Most existing studies on formation problems predominantly address ideal environments with simplistic systems, often overlooking the uncertainties and disturbances inherent in the formation systems. Hence, it becomes imperative to explore the formation of multiple UAV systems in the context of these uncertainties and disturbances[26]. Existing literature proposes a variety of control methods to resist the influence of uncertain disturbance on UAV formation control, such as sliding control[24], fuzzy control[27], neural network control[28], and robust control[29]. Wang et al.[30] designed a disturbance-based observation to compensate for external disturbances and established a sliding film control model within a consecutive time to achieve the formation of drones in an uncertain environment. Zhang and Yan[31] proposed a novel control strategy for three fixed-wing unmanned aerial vehicle formation flights with wind fields, ensuring precise air-to-ground strikes. The integrated controller establishes a theoretical framework to maintain UAV formation geometry and achieve stable and robust consensus control. Islam et al.[32] proposed an adaptive input algorithm for autonomous flight control of a quadrotor unmanned flying robot vehicle with the help of an energy function, which can guarantee asymptotic stability and tracking. Liu et al.[33] presented a distributed robust controller that encompasses both a position controller for managing the translational motion of the desired formation and an attitude controller for regulating the rotational motion of each quadrotor. Zhao et al.[34] presented a formation controller for quadrotors using a hierarchical control scheme and reinforcement learning.

Inspired by robust control methods[35, 36], we investigate the formation challenges faced by multi-UAVs in uncertain environments. In response, we introduce a distributed robust control strategy aimed at enhancing the stability and robustness of the UAV formation system. In this paper, we only need to use the local information of UAVs (relative positions and velocities) to converge to the expected formation under the proposed robust control strategy. Specifically, we initially present a nominal control strategy grounded in positional relationships for UAVs adhering to a single

integrator model. Subsequently, we formulate a semi-definite programming model to determine the control gains within this strategy. To address the noise and disturbance in the system, we propose a robust control strategy under the rotation set Ω and prove the convergence and robustness of the UAV control system. Even when the rotation angles of the UAVs change, they still move towards the expected direction and form a stable formation. Furthermore, we extend the proposed robust control strategy to a quadrotor unmanned aerial vehicle system with high-order kinematic models. Finally, we apply the proposed control strategy to a group of quadrotor unmanned aerial vehicle systems and conduct simulation experiments. The results show that the UAV swarm can resist uncertain disturbances and form a stable formation under two different simulation environments. The contributions of our work are summarized as follows:

- In this paper, a distributed robust control strategy is proposed to improve the stability and robustness of multi-UAV formation systems in uncertain environments. Under this control strategy, UAVs can autonomously form a desired formation based on local information.
- To counteract system noise and disturbances, we introduce a novel robust control strategy based on the rotation set Ω. This approach guarantees the convergence and robustness of the UAV control system, ensuring that UAVs maintain their intended trajectory and achieve a stable formation, even amidst varying rotation angles.
- The proposed control strategy is extended to a quadrotor unmanned aerial vehicle system with high-order kinematic models. Through simulation tests across two distinct environments, it is evident that the UAV swarm effectively counteracts uncertain disturbances, consistently achieving a stable formation.

The organisational structure of this paper is as follows. In Section 2, we introduced the robust control architecture for UAVs under a single-integrator model and a new control gain based on semidefinite programming is presented. In Section 3, we extended the proposed control strategy to a UAV system with higher-order linear dynamics and applied the gains under the single integrator to this higher-order system. Next, we conduct simulation experiments in Section 4 to typify the robust control strategy for the UAVs formation system. Specifically, we present the experimental results, perform parametric analysis, and perform experimental comparisons. Finally, we concluded the paper and illustrated future work in Section 5.

2 Robust Control Architecture under Single-Integrator Model

In this section, we focus on designing a distributed robust controller tailored for each UAV i, where i belongs to set $\mathcal{I}$, to facilitate stable platoon formation amidst uncertain conditions. As shown in Fig. 1, we depict the system scenario and an implementation framework of a robust control approach for UAV swarm. The robust control method is conceptualized to address the inherent uncertainties and external disturbances that the UAV swarm might encounter during its operations. Firstly, based on the two-dimensional (2D) initial position information and the desired formation information of UAV swarms, we propose closed-loop dynamic equations for UAVs under interference. Then, we employ a semi-definite program (SDP) model to determine the control gain matrix G under the rotation set Ω. Leveraging uncertain rotation matrices, we further devise a position-centric robust control approach. The notations are summarized in Table 1.

2.1 Nominal control strategy of UAVs

In this section, we introduce a nominal control strategy for a UAV swarm without external perturbations. According to Refs. [34] and [35], the single-integral model is able to provide a mathematically feasible and computationally satisfying expression for UAV's motion. For simplicity, the set of the UAVs is denoted by $\mathcal{N} = \{1, 2, \ldots, n\}$. For the UAV i, the single-integrator dynamic equation has the following form

$$\dot{s}_i = u_i, i \in \mathcal{N} \tag{1}$$

where $s_i = [x_i, y_i]^{\mathrm{T}} \in \mathbb{R}^2$ is the 2D coordinate of UAV i and u_i is the control signal of the UAV i. In order to make the UAV reach the pre-set formation configuration, we adopt the following control strategy

$$u_i = \sum_{j \in \mathcal{N}_i} g_{ij}\left(s_j - s_i\right) \tag{2}$$

where $g_{ij} \in \mathbb{R}^{2\times 2}$ is the gain matrix under control strategy Eq. (2) and s_j is the 2D coordinate of UAV j. g_{ij} is a constant matrix, and its solution will be explained in detail later. Usually, its expression is

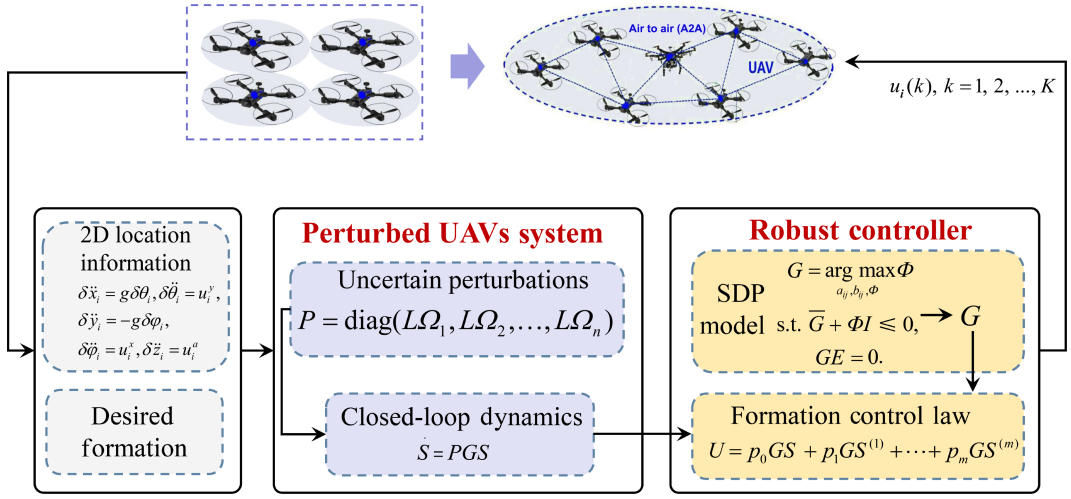

Fig. 1 System scenario and implementation framework of robust control approach for UAV swarm.

Table 1 Basic notations in this paper.

Symbol	Description
$\mathcal{N} = \{1,2,\ldots,n\}$	Set of UAVs
$\mathcal{N}_i$	Subset of $\mathcal{N}$ which includes neighbors of i
$\mathcal{G} = (\mathcal{V}, \mathcal{E})$	Undirected graph
$\mathcal{V}$	Set of vertices
$\mathcal{E}$	Set of edges
$[x_i, y_i]$	Coordinate of UAV i
u_i	Control variables of UAV $i, i \in \mathcal{N}$

Note: [1]If UAV i and UAV j obtain each other's position information in the coordinate system, then UAV i and j are called neighbours.
[2]The subset $\mathcal{N}_i = \{j \in \mathcal{V} | (i,j) \in \mathcal{E}\}$

$$g_{ij} = \begin{bmatrix} a_{ij} & b_{ij} \\ -b_{ij} & a_{ij} \end{bmatrix}, \quad a_{ij} \text{ and } b_{ij} \in \mathbb{R} \tag{3}$$

Based on the research conducted by Refs. [37, 38], it has been demonstrated that the information obtained in the local coordinate system, namely s_j and s_i, is consistent with the information obtained in the global coordinate system. As a result, even when we obtain the local relative position of the UAV under the distributed control strategy, the strategy can still be applied and analyzed in the global coordinate system.

For all UAVs, we define the composite state and control vectors as

$$\begin{aligned} S &= \left[s_1^{\mathrm{T}}, s_2^{\mathrm{T}}, \ldots, s_i^{\mathrm{T}}, \ldots, s_n^{\mathrm{T}}\right], S \in \mathbb{R}^{2n}; \\ U &= \left[u_1^{\mathrm{T}}, u_2^{\mathrm{T}}, \ldots, u_i^{\mathrm{T}}, \ldots, u_n^{\mathrm{T}}\right], U \in \mathbb{R}^{2n} \end{aligned} \tag{4}$$

Thus, the closed-loop dynamics equation of the UAV swarm can be deduced as

$$\dot{S} = GS \tag{5}$$

where gain matrix $G \in \mathbb{R}^{2n \times 2n}$ and

$$G = \begin{bmatrix} -\sum_{j=2}^{n} g_{1j} & g_{12} & \cdots & g_{1n} \\ g_{21} & -\sum_{\substack{j=1 \\ j \neq 2}}^{n} g_{2j} & \cdots & g_{2n} \\ \vdots & \vdots & \ddots & \vdots \\ g_{1n} & g_{2n} & \cdots & -\sum_{j=1}^{n-1} g_{nj} \end{bmatrix} \tag{6}$$

Note that when j does not belong to UAV i's neighbour set $\mathcal{N}_i$, then all elements in g_{ij} are 0. Furthermore, every 2×2 matrix on the diagonal in G is equal to the negative of the sum of the other matrices. Since G has the block Laplacian structure, define the following vectors:

$$\begin{aligned} \mathcal{L}_1 &= [1,0,1,0,\ldots,1,0]^{\mathrm{T}} \in \mathbb{R}^{2n}, \\ \mathcal{L}_2 &= [0,1,0,1,\ldots,0,1]^{\mathrm{T}} \in \mathbb{R}^{2n} \end{aligned} \tag{7}$$

where $\mathcal{L}_1$ and $\mathcal{L}_2$ satisfy $\mathcal{L}_1 G = 0$ and $\mathcal{L}_2 G = 0$, therefore, $\mathcal{L}_1$ and $\mathcal{L}_2$ are in the kernel of G.

Let S^* denote the ideal coordinates of all UAVs in the desired formation, i.e., $S^* = [s_1^{*\mathrm{T}}, s_2^{*\mathrm{T}}, \ldots, s_i^{*\mathrm{T}}, \ldots, s_n^{*\mathrm{T}}]$. $\overline{S}^*$ denotes the coordinate of UAVs when the rotation angle of this desired formation around the origin is a right angle, i.e., $\overline{S}^* = [\overline{s}_1^{*\mathrm{T}}, \overline{s}_2^{*\mathrm{T}}, \ldots, \overline{s}_i^{*\mathrm{T}}, \ldots, \overline{s}_n^{*\mathrm{T}}]$. To ensure that the UAV swarm converges to the desired formation, the gain matrix G should satisfy two conditions[33]: (1) $\mathcal{L}_1$, $\mathcal{L}_2$, S^*, and $\overline{S}^*$ are in the kernel of G; (2) except for the four zero eigenvalues associated with these empty vectors, all other eigenvalues of G contain negative real parts.

2.2 Control gain design

Suppose S^* is the coordinate information of all UAVs in the desired formation, $\overline{S}^*$ is the coordinate information after rotating 90 degrees around the origin, 1 and $\overline{1}$ are given by Eq. (7), and the definition set $E=[S^*,\overline{S}^*,1,\overline{1}]$. In addition, rewrite E as a singular value decomposition form:

$$E=CQV^{\mathrm{T}},\ C=[\overline{R},R] \tag{8}$$

where Q is a diagonal matrix and the diagonal elements are singular values of the matrix E. The transpose of V is an orthogonal matrix. $R\in\mathbb{R}^{2n\times(2n-4)}$ is the last $2n-4$ columns of C.

In this decomposition form of Eq. (8), it can be inferred that both G and $\overline{G}=R^{\mathrm{T}}GR$ possess identical non-zero characteristic terms. Next, we proceed to solve $f(G)$ using the fastest mixed Markov process approach[39]. When given an undirected graph $\mathcal{G}$, we consider its Markov process in continuous time, where the state transition probabilities of UAV i at time t are described by the probability density function $\Pr(t)$. The $\Pr(t)$ is

$$\Pr(t)=\Pr(0)\mathrm{e}^{-t\mathcal{L}} \tag{9}$$

where $\Pr(0)$ represents the probability density vector of the initial state, and $\mathcal{L}$ is the Laplacian matrix of the graph $\mathcal{G}$. We can observe that the probability density decays exponentially with time t, and when $t\to+\infty$, the probability distribution tends to a stable equilibrium state (uniform distribution). According to Ref. [40], the convergence speed of $\Pr(t)$ to uniform distribution is determined by the smallest positive eigenvalue $\lambda_G(G)$ of the Laplacian matrix. Specifically, smaller values of $\lambda_G(G)$ indicate a faster convergence of the Markov process towards a uniform distribution. Therefore, in order to achieve the fastest convergence speed, we pose the model M1.

$$\begin{aligned}&\min_{a_{ij},b_{ij}}\ \lambda_G(G)\\&\text{s.t.},\ GE=0,\\&\mathrm{trace}(G)=\text{constant}\end{aligned} \tag{10}$$

In order to effectively eliminate the 0 eigenvalues of G, we adopt the projection $\overline{G}=R^{\mathrm{T}}GR$, and then the problem M1 can be transformed into maximisation model M2.

$$\begin{aligned}&G=\arg\max_{a_{ij},b_{ij}}\lambda_G(-\overline{G})\\&\text{s.t.},\ GE=0,\\&\mathrm{trace}(G)=\text{constant}\end{aligned} \tag{11}$$

where $f(\cdot)$ represents the smallest eigenvalue of the matrix. The model Eq. (11) is a concave maximization problem[41], and then we transform it into an SDP model

$$\begin{aligned}&G=\arg\max_{a_{ij},b_{ij},\Phi}\ \Phi\\&\text{s.t.},\ \overline{G}+\Phi I\leqslant 0,\\&GE=0,\\&\mathrm{trace}(G)=\text{constant}\end{aligned} \tag{12}$$

where Φ is a new decision variable and I is unit matrix.

Then, we transform the original concave optimization model Eq. (11) into an SDP model, which is an epigraph optimization model. The SDP model can be solved through existing algorithms specifically designed for solving SDP problems.

Remark 1 By $\overline{G}=R^{\mathrm{T}}GR$, it can be observed that the set E is an orthogonal matrix, and $\mathrm{range}(\overline{R})=\mathrm{range}(E)$. Therefore, we can deduce that $\overline{G}$ restricts the orthogonal complement of G in the $\mathrm{range}(E)$ and eliminates the 0 eigenvalues in G. This also shows that the non-zero eigenvalues of $\overline{G}$ and G are equivalent.

2.3 Robust control under rotation set Ω

In practical control systems, disturbances such as white noise and uncertain parameters often exist. These uncertainties can significantly affect the control system's performance, leading to undesired behaviour or even instability. To address this issue, a robust control strategy is proposed in this study. In practical control systems, disturbances like white noise and uncertain parameters frequently arise. Such uncertainties can profoundly impact the performance of the control system, potentially causing undesirable behaviour or even system instability. To tackle these challenges, this study introduces a robust control strategy. The proposed strategy enables all drones to move along the desired trajectory even under uncertain disturbances and ultimately form the desired formation. Based on this, we propose an uncertain rotation set Ω and develop a corresponding robust control strategy under this set. We prove the stability and convergence of this strategy under disturbances.

Theorem 1 If radian parameter $\alpha\in\left[-\frac{\pi}{2}+\epsilon,\frac{\pi}{2}-\epsilon\right]$ with an arbitrarily small $\epsilon>0$, and there exists a constant $L>0$, the rotation set Ω is defined as the following form:

$$\Omega=\begin{bmatrix}\cos(\alpha) & -\sin(\alpha)\\ \sin(\alpha) & \cos(\alpha)\end{bmatrix} \tag{13}$$

Based on this rotation set Ω, the robust control

strategy of UAV i can be designed as

$$u_i = L\Omega_i \sum_{j\in\mathcal{N}_i} g_{ij}\left(s_j - s_i\right) \tag{14}$$

where Ω_i is a rotation matrix of UAV i, and all UAVs under the single-integrator dynamics can achieve the desired formation.

Proof For all UAVs, the closed-loop dynamics system can be deduced as

$$\dot{S} = PGS \tag{15}$$

where P is a perturbation matrix which has the following form:

$$P = \mathrm{diag}(L\Omega_1, L\Omega_2, \ldots, L\Omega_n) \in \mathbb{R}^{2n\times 2n} \tag{16}$$

Assumed that the Lyapunova function is $V = -U^{\mathrm{T}}GU$. Due to the gain matrix G being negative semidefinite, the Lyapunov function V is positive semidefinite. This means that $V = 0$ if and only if $U \in \ker(G)$. Next, the derivative of V is

$$\begin{aligned}\dot{V} =& -\dot{U}^{\mathrm{T}}GU - U^{\mathrm{T}}G\dot{U} = \\ & -U^{\mathrm{T}}G\left(P^{\mathrm{T}} + P\right)GU\end{aligned} \tag{17}$$

For the rotation set Ω_i in P, we can deduce

$$\Omega_i + \Omega_i^{\mathrm{T}} = \begin{bmatrix} \cos(\alpha_i) & 0 \\ 0 & 2\cos(\alpha_i) \end{bmatrix} \tag{18}$$

when $|\alpha_i| < \dfrac{\pi}{2}$ and $L > 0$, the matrix $\Omega + \Omega^{\mathrm{T}}$ is positive definite. Furthermore, $(P^{\mathrm{T}} + P)$ is also block diagonal and positive definite. If all $U \notin \ker(\mathrm{G})$, $\dot{V} < 0$. According to LaSalle's invariance principle[42], the trajectories of $\dot{S} = PGU$ converge to the $\ker(G)$, which shows that even in the presence of uncertain disturbances, the robust control strategy Eq. (14) can still ensure that all UAVs achieve the desired formation. ■

3 Control Architecture under Higher-Order Model

Suppose the state matrix of UAV i with m-order dynamics ($m > 2$) system is

$$X_i = [S, S^{(1)}, \ldots, S^{(m-1)}, S^{(m)}] \tag{19}$$

and its m-order derivative is

$$X_i^{(m)} = [\dot{S}, \dot{S}^{(1)}, \ldots, \dot{S}^{(m-1)}, \dot{S}^{(m)}] \tag{20}$$

Thus the compact form of UAVs' dynamics can be deduced as

$$X_i^{(m)} = M_1 X_i + M_2 U \tag{21}$$

where

$$M_1 = \begin{bmatrix} 0 & I & 0 & \cdots & 0 \\ 0 & 0 & I & \cdots & 0 \\ \vdots & \vdots & \vdots & \ddots & \vdots \\ 0 & 0 & 0 & \cdots & I \\ 0 & 0 & 0 & \cdots & 0 \end{bmatrix},\ M_2 = \begin{bmatrix} 0 \\ 0 \\ \vdots \\ 0 \\ I \end{bmatrix} \tag{22}$$

Based on the control gain G obtained by the SDP model Eq. (12) and robust controller Eq. (14) designed in Section 3, the robust control strategy of the UAV swarm can be written as

$$U = p_0 GS + p_1 GS^{(1)} + \cdots + p_m GS^{(m)} \tag{23}$$

where $p_0, p_1, \ldots, p_m$ are the scalar control gains, which are related to the uncertain rotation set and L[43]. Thus, the state equation of UAVs can be written as

$$X_i^{(m)} = MX_i \tag{24}$$

where

$$M = \begin{bmatrix} 0 & I & 0 & \cdots & 0 \\ 0 & 0 & I & \cdots & 0 \\ \vdots & \vdots & \vdots & \ddots & \vdots \\ 0 & 0 & 0 & \cdots & I \\ p_0 G & p_1 G & p_2 G & \cdots & p_m G \end{bmatrix} \tag{25}$$

Next, we will demonstrate that a robust control strategy for m-order dynamic systems can ensure that all UAVs achieve the desired displacement.

Theorem 2 Suppose the polynomial function $f(\alpha)$ is

$$f(\alpha) = \lambda^{m+1} - p_m\alpha\lambda^m - \cdots - p_1\alpha\lambda - p_0\alpha \tag{26}$$

where λ is an eigenvalue. When $f(\alpha) = 0$, all nonzero roots $\alpha \in \ker(G)$ have negative real parts. Under the robust control strategy, the UAVs with dynamics Eq. (24) have global convergence which shows that all UAVs can achieve the desired formation.

Proof By observing Eq. (24), it can be found that M is a controllable canonical matrix. According to Ref. [43], its characteristic equation can be written as

$$\lambda^{m+1} I - p_m\lambda^m G - \cdots - p_1 G - p_0 G = 0 \tag{27}$$

Thus, the eigenvalues of G have the negative real part. The m-order dynamic system $X_i^{(m)} = MX_i$ converges to the $\ker(G)$, which shows that even in the presence of uncertain disturbances, the robust control strategy Eq. (23) can still ensure that all UAVs achieve the desired formation.

4 Simulation Experiment

In order to validate the effectiveness of the proposed

control method, we conduct simulations of the UAV platforming in two distinct scenarios. Furthermore, we investigate the impact of the gain parameter p_m on the system's stability. Lastly, a comparative analysis is conducted to verify the robustness of the control strategy. In addition, all simulations of the proposed control method are implemented using a combination of MATLAB modelling toolbox and convex programming solver. The convex programming solver can be used to solve the SDP model Eq. (12) through a specific interface in MATLAB to obtain the gain G. This program is run on 2.8 GHz 64-bit Core i5-8400U CPU machine under Windows 10 Professional.

4.1 Simulation result

In this section, we present a 2D state equation of the UAV dynamics system[44]. Specifically, we only consider the lateral dynamics of the UAV along x- and y-axis and assume that the height (z-axis) of the drone in space is fixed. Thus, the 2D state vector is: $X_i = [x_i, y_i, \dot{x}_i, \dot{y}_i, \theta_i, \varphi_i, \dot{\theta}_i, \dot{\varphi}_i]^{\mathrm{T}}$, and the control vector is: $U_i = [u_i^y, u_i^x]^{\mathrm{T}}$. The corresponding state equation has the following form

$$\dot{X}_i = \begin{bmatrix} 0 & I & 0 & 0 \\ 0 & 0 & I & 0 \\ 0 & 0 & 0 & I \\ 0 & 0 & 0 & 0 \end{bmatrix} X_i + \begin{bmatrix} 0 \\ 0 \\ 0 \\ I \end{bmatrix} U_i \tag{28}$$

where $I \in \mathbb{R}^{2n \times 2n}$. Based on the state equation, we design two desired formation cases for different numbers of UAVs.

Scenario 1: We perform a simulation on a small-scale swarm of 4 UAVs, defining the final desired platoon as a square. The robust control strategy of Scenario 1 is $U_i^1 = p_0 G X_i + p_1 G \dot{X}_i$. The control gain G can be solved by model Eq. (12) and parameters $p_0 = 0.1$ and $p_1 = 1.0$.

Scenario 2: We simulate a large-scale swarm of 9 UAVs and define the final desired arrangement as a square grid shape. The control strategy of Scenario 2 is $U_i^2 = p_0 G X_i + p_1 G \dot{X}_i + p_2 G \ddot{X}_i + p_3 G \dddot{X}_i$. Note that the control gain G is obtained by calculating the SDP model, which ensures the stability and robustness of the platoon; the value range of G is $[0.72, -10.00]$ and $p_0 = 0.1$, $p_1 = 1.0$, $p_2 = 0.8$, and $p_3 = 1.0$.

The robust control algorithm is summarized in Algorithm 1. Next, we demonstrate the formation effects of the proposed robust control strategy in two distinct scenarios. Figures 2 and 3 provide top-down views of the UAVs at distinct time intervals across two different scenarios, with the perception topology among the UAVs depicted using grey lines. In Fig. 2, the dynamic trajectories of 4 UAVs are captured over four time instances. Beginning with their initial positions in Fig. 2a, the UAVs transition towards their target square formation, as portrayed progressively in Figs. 2b–2d, under the influence of the robust control strategy. Conversely, Fig. 3 presents the evolution of a group of 9 UAVs in Scenario 2. The starting positions of each UAV, complemented by their perception topology, are highlighted in Fig. 3a. Figures 3b–3h sequentially depict the UAVs' movements at various moments. Notably, under the control strategy U_i^2, all UAVs can follow the intended trajectory, culminating in a well-defined square grid formation.

Algorithm 1 Control algorithm of UAV swarm

Input: The desired formation coordinates S^*; the scalar control gains p_m; the initial coordinates of all UAVs; simulation time T.

1. Construct the m-order state equation;
2. Let $E = [S^*, \overline{S}^*, 1, \overline{1}]$;
3. Decompose E: $E = CQV^{\mathrm{T}}$, $C = [\overline{R}, R]$;
4. Define R is the last $2n-4$ columns of C;
5. Compute the gain matrix G by SDP model Eq. (10);
6. Generate the control signal:
$U = p_0 GS + p_1 GS^{(1)} + \cdots + p_m GS^{(m)}$

Output: The global coordinates, velocity, and relative distance of UAVs.

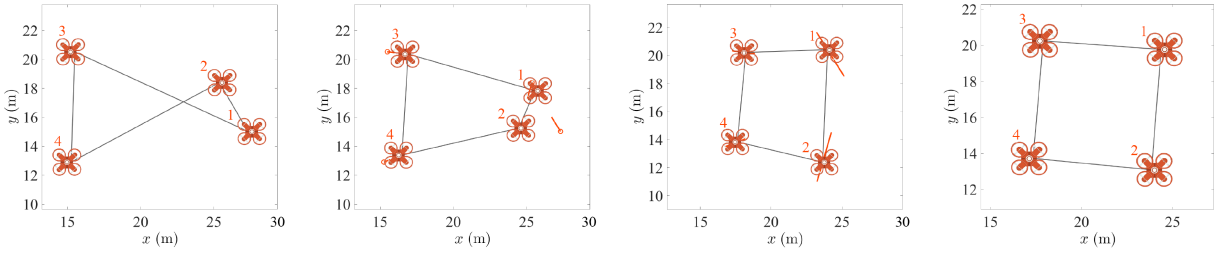

(a) $t = 0$ s (b) $t = 4$ s (c) $t = 15$ s (d) $t = 33$ s

Fig. 2 Coordinate information (x-axis and y-axis) of the 4 UAVs when the expected formation is a square (Scenario 1).

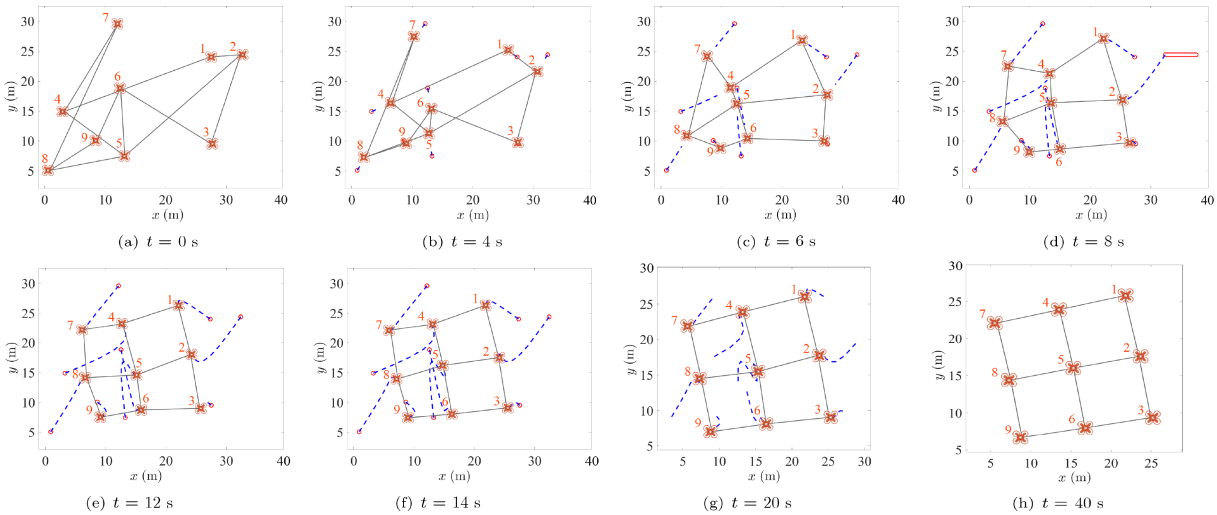

Fig. 3 Coordinate information (*x*-axis and *y*-axis) of the 9 UAVs when the expected formation is a square grid (Scenario 2).

Furthermore, Figs. 4 and 5 depict the velocities, encompassing both angular and linear velocities, of all the UAVs in two distinct scenarios. Figures 4a–4d present the angular and linear velocities of the 4 UAVs with respect to the time variable t. It is evident that the drones progressively establish the desired square formation at approximately 3 s, followed by formation adjustment and convergence towards a stable state. Similarly, Figs. 5a–5d showcase the angular and linear velocities of the 9 UAVs in relation to the time variable t. All the drones successfully achieve the desired formation within the time interval $[7, 8]$ s and subsequently converge to a stable state, ultimately forming a square-shaped configuration.

Besides, we demonstrate the relative distances between UAVs in two different scenarios in Figs. 6 and 7, where $d_{1,2}$ represents the distance between UAV 1 and UAV 2. From Fig. 6, it can be observed that the distances between the four drones gradually converge to a stable spacing of 7.434 m as they form the desired square formation over time. Similarly, Fig. 7 shows that the distances between the nine UAVs gradually converge to a stable spacing of 8.235 m as they form the desired line formation.

4.2 Parametric analysis

In this section, we explore the effect of the gain parameter p_m on the stability and safety of the formation system. For observation purposes, we simulate a large-scale swarm consisting of 9 UAVs

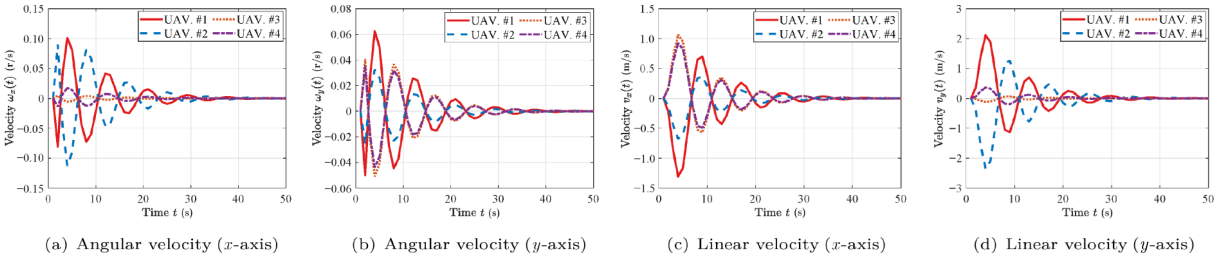

Fig. 4 Velocity (*x*-axis and *y*-axis) of the 4 UAVs in Scenario 1.

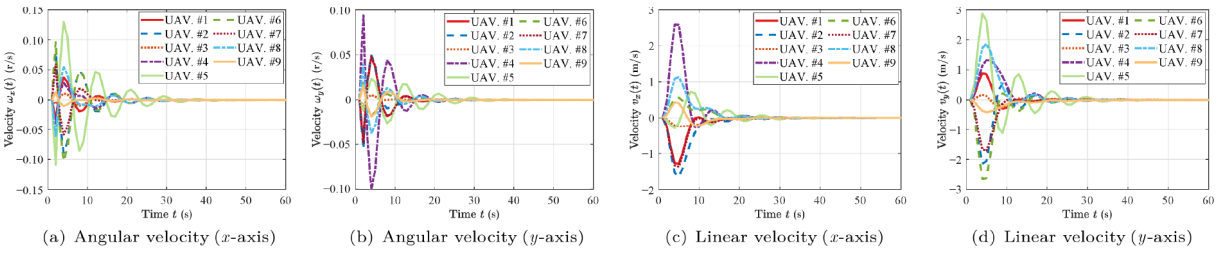

Fig. 5 Velocity (*x*-axis and *y*-axis) of the 9 UAVs in Scenario 2.

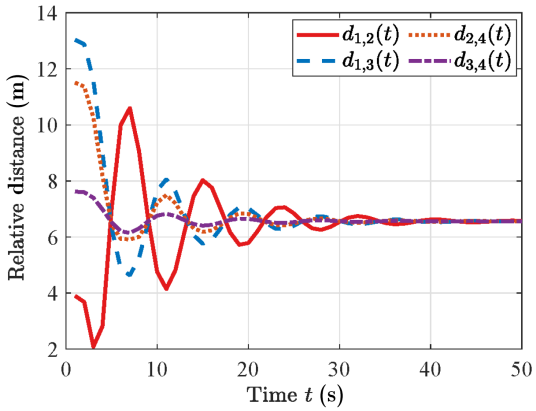

Fig. 6 Relative distance of 4 UAVs in Scenario 1.

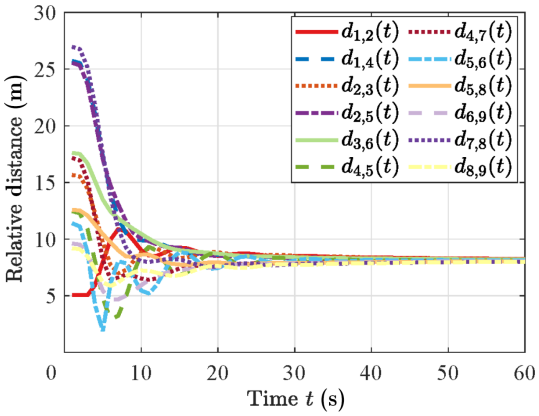

Fig. 7 Relative distance of 9 UAVs in Scenario 2.

under Scenario 2. Specifically, the gain parameter p_m is taken in the following four cases:

Case 1: $p_0 = 0.1$, $p_1 = 5.0$, $p_2 = 5.0$, and $p_3 = 1.0$;

Case 2: $p_0 = 0.1$, $p_1 = 0.9$, $p_2 = 5.0$, and $p_3 = 2.0$;

Case 3: $p_0 = 0.1$, $p_1 = 5.0$, $p_2 = 2.3$, and $p_3 = 5.0$;

Case 4: $p_0 = 0.1$, $p_1 = 5.0$, $p_2 = 5.0$, and $p_3 = 5.0$.

Figure 8 visually presents the velocities of nine UAVs forming a structured square grid formation with different gain parameters, encompassing both angular and linear velocities. The selection of parameter p_m notably influences the stability of the formation system. It is evident that under Case 1, the UAV velocities exhibit instability, failing to meet the required velocity consistency for formation. However, in Case 4, the angular velocity of the UAVs begins to stabilize at 40 s, and the linear velocity of the UAVs starts to stabilize at 15 s. Moreover, Fig. 9 depicts the relative distances between each pair of connected UAVs, clearly illustrating that the choice of the gain parameter in Case 4 enhances the overall stability of the formation shaping system.

4.3 Comparative experiment

In this section, we compare the proposed SDP gain-based robust control strategy with the linear feedback control (LF control) strategy in two scenarios. In our proposed method, the control strategy (SDP-based control) is $U = p_0GS + p_1GS^{(1)} + \cdots + p_mGS^{(m)}$. The linear feedback control is $U = KX = K_1S + K_2S^{(1)} + \cdots + K_mS^{(m)}$, where K is gain matrix.

Figure 10 presents the ultimate formation configuration of the four UAVs in Scenario 1, along with the relative distance error bands encompassing the entire formation system. As depicted in Figs. 10a and 10b, it is evident that the UAVs, employing both control strategies, successfully achieve the desired formation. However, it is noteworthy that the distance error between the UAVs progressively increases under the LF control method (Fig. 10d), whereas the error band under the SDP control method converges to zero after 30 s, underscoring the effectiveness of the proposed control approach. Similarly, Fig. 11 illustrates the ultimate formation configuration and relative distance error bands of the nine UAVs in Scenario 2. Notably, Figs. 11a and 11b clearly depict that the 9 UAVs operating under the LF control method fail to achieve the intended arrangement, specifically the square grid shape. In contrast, the UAVs under the SDP-based control method successfully establish a stable formation. Subsequently, as evident in Figs. 11c and 11d, the spacing error among the nine UAVs under the SDP-based control method gradually converges to 0, while the distance error under the LF control method progressively increases, ultimately preventing the UAVs from attaining the desired formation.

Furthermore, Table 2 presents the average relative distance error and the corresponding standard deviation between interconnected UAVs for various control methods and scenarios throughout the entire time system. Remarkably, when compared, the proposed SDP-based control method exhibits a smaller standard deviation across different scenarios in comparison to the LF control method. This observation highlights the enhanced robustness and system safety assurance provided by the SDP-based control method.

Finally, in order to verify the superiority of the proposed robust control strategy, we conduct an expansion experiment in which the UAV swarm size is scaled up to $n = 12$. Figure 12 shows the switching trajectories of 12 UAVs under 6-time slots, from which

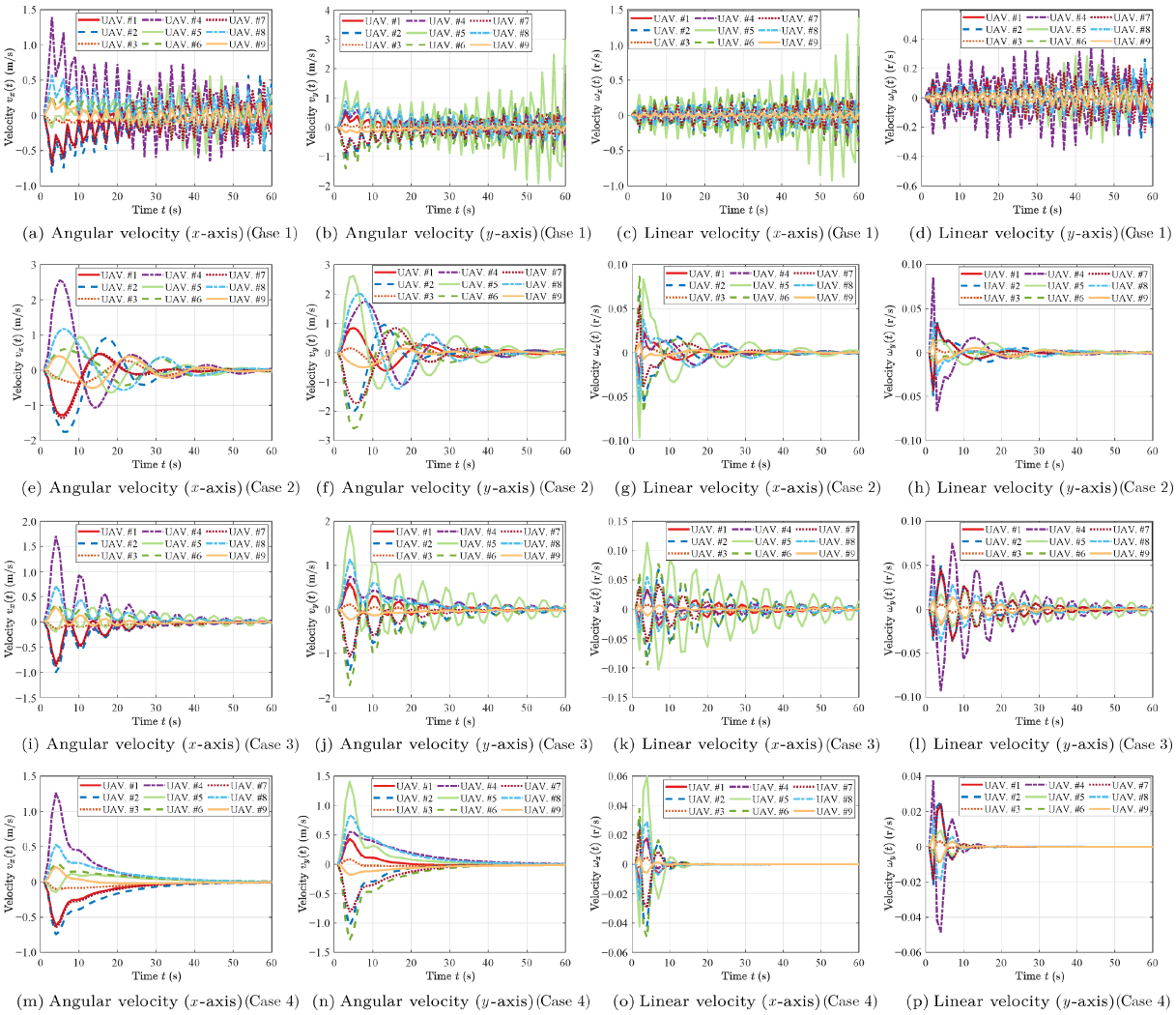

(a) Angular velocity (x-axis) (Case 1) (b) Angular velocity (y-axis) (Case 1) (c) Linear velocity (x-axis) (Case 1) (d) Linear velocity (y-axis) (Case 1)

(e) Angular velocity (x-axis) (Case 2) (f) Angular velocity (y-axis) (Case 2) (g) Linear velocity (x-axis) (Case 2) (h) Linear velocity (y-axis) (Case 2)

(i) Angular velocity (x-axis) (Case 3) (j) Angular velocity (y-axis) (Case 3) (k) Linear velocity (x-axis) (Case 3) (l) Linear velocity (y-axis) (Case 3)

(m) Angular velocity (x-axis) (Case 4) (n) Angular velocity (y-axis) (Case 4) (o) Linear velocity (x-axis) (Case 4) (p) Linear velocity (y-axis) (Case 4)

Fig. 8 Velocity (x-axis and y-axis) of 9 UAVs under different p_m.

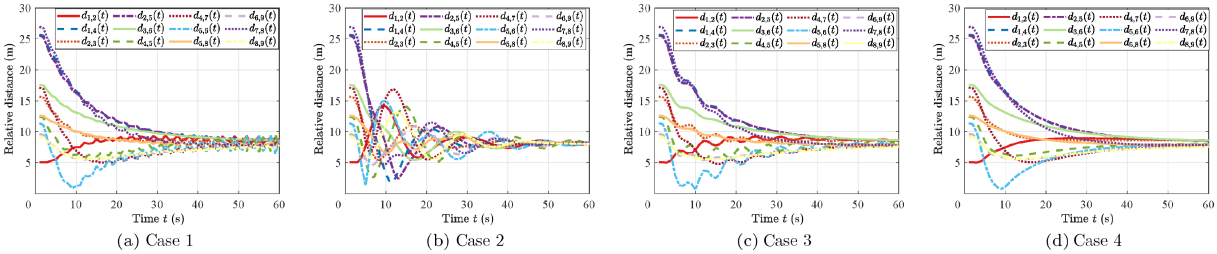

(a) Case 1 (b) Case 2 (c) Case 3 (d) Case 4

Fig. 9 Relative distance of 9 UAVs under different p_m.

it can be seen that the UAVs start from the initial position (Fig. 12a) and move towards the desired square under the proposed robust control strategy (Figs. 12b−12e). Eventually, all UAVs form a rectangular network-like formation. In addition, we compute the relative distance between 12 UAVs in Fig. 13, where $d_{4,7}$ represents the distance between UAV 4 and UAV 7. We can observe that as the UAV swarms form a triangular formation, the distance between them gradually converges to a stable spacing of 7.267 m. Besides, Table 3 shows the execution time of the proposed robust algorithm method for the UAVs. As can be seen, the formation of 12 UAVs can be computed in less than 0.3000 s.

5 Conclusion

In this study, we presented a robust formation control method for UAV swarms to ensure stability and

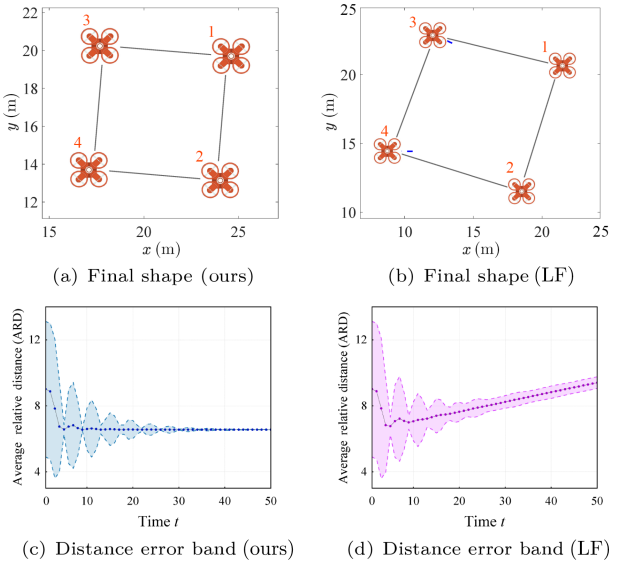

(a) Final shape (ours) (b) Final shape (LF)

(c) Distance error band (ours) (d) Distance error band (LF)

Fig. 10 Comparative experiments of 4 UAVs under different control strategies. SDP-based control (left) and LF control (right).

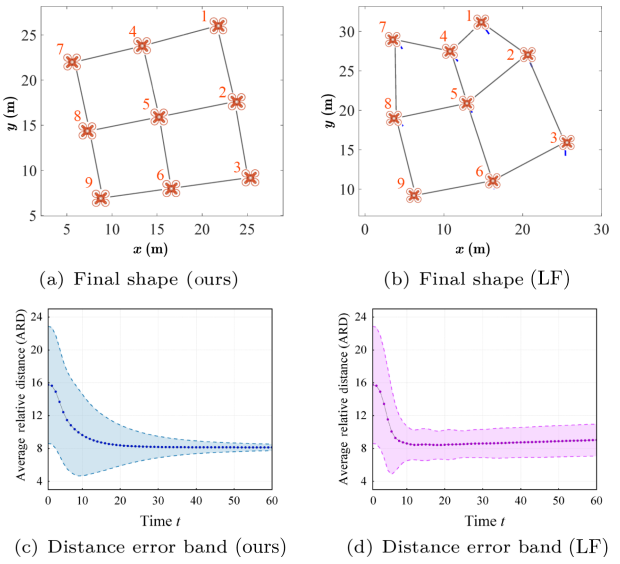

(a) Final shape (ours) (b) Final shape (LF)

(c) Distance error band (ours) (d) Distance error band (LF)

Fig. 11 Comparative experiments of 9 UAVs under different control strategies. SDP-based control (left) and LF control (right).

Table 2 Mean (Avg.) and standard deviation (Std.) of the relative distance between UAVs for SDP-based control and LF control.

Scenario	Relative distance (m)			
	SDP-based control		LF control	
	Avg.	Std.	Avg.	Std.
1	6.701	0.665	8.113	0.873
2	8.942	2.235	9.184	2.846

robustness during formation flight. Relying on an undirected topology, a position-based feedback control

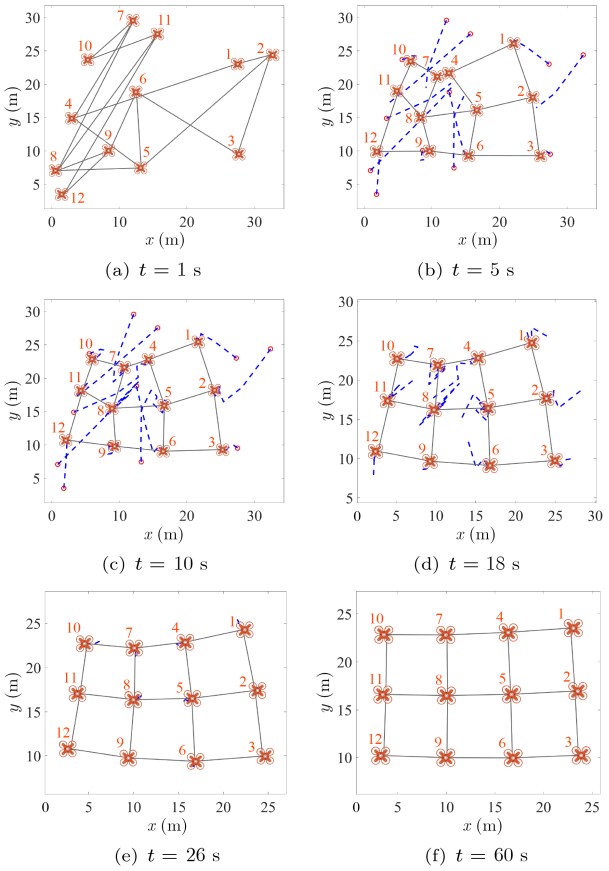

(a) $t = 1$ s (b) $t = 5$ s

(c) $t = 10$ s (d) $t = 18$ s

(e) $t = 26$ s (f) $t = 60$ s

Fig. 12 Coordinate information (*x*-axis and *y*-axis) of the 12 UAVs when the expected formation is rectangular.

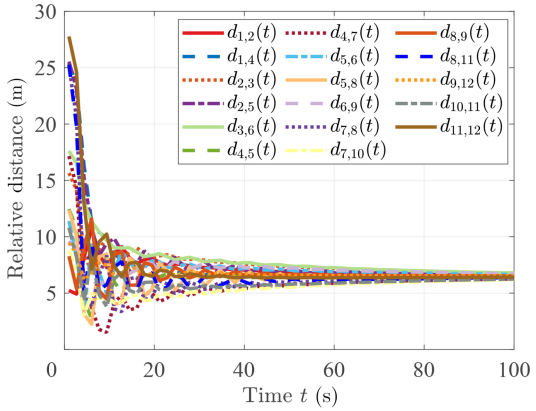

Fig. 13 Relative distance of 12 UAVs.

Table 3 Execution time of robust control algorithm.

Scenario	Number of UAVs		
	4 UAVs	9 UAVs	12 UAVs
SDP-based time	0.0411 s	0.0860 s	0.2486 s

strategy was introduced. Within this strategy, the control gain is determined by solving an SDP model. Recognizing the challenges posed by noise interference in uncertain environments, we also proposed and

proved a robust control strategy under uncertain rotation sets that ensured the convergence of all UAVs to the desired formation. Simulation experiments were conducted to validate the effectiveness of the proposed control strategy. Our research contributed to the advancement of robust control methods for UAV swarms, showcasing potential applications in areas such as search and rescue, monitoring, and transportation. Our future work will centre on enhancing UAV-to-UAV communication to avert collisions during platoon formation. Furthermore, we intend to explore the reliability of such communications, aiming to uphold both the stability of UAV formation and communication reliability.

Acknowledgment

This work was supported by the National Natural Science Foundation of China (Nos. 52202391, U20A20155, and 52302397) and the China Postdoctoral Science Foundation (No. 2023M730173).

References

[1] Y. Liu, J. M. Montenbruck, D. Zelazo, M. Odelga, S. Rajappa, H. H. Bulthoff, F. Allgower, and A. Zell, A distributed control approach to formation balancing and maneuvering of multiple multirotor UAVs, *IEEE Trans. Robot.*, vol. 34, no. 4, pp. 870–882, 2018.

[2] A. Hegde and D. Ghose, Multi-UAV distributed control for load transportation in precision agriculture, in *Proc. AIAA Scitech 2020 Forum*, Orlando, FL, USA, 2020, p. 2068.

[3] A. Gupta, T. Afrin, E. Scully, and N. Yodo, Advances of UAVs toward future transportation: The state-of-the-art, challenges, and opportunities, *Future Transp.*, vol. 1, no. 2, pp. 326–350, 2021.

[4] P. Zhang, Y. Liu, G. Yang, and G. Zhang, A multi-objective distributionally robust model for sustainable last Mile relief network design problem, *Ann. Oper. Res.*, vol. 309, no. 2, pp. 689–730, 2022.

[5] A. Ryan, M. Zennaro, A. Howell, R. Sengupta, and J. K. Hedrick, An overview of emerging results in cooperative UAV control, in *Proc. 2004 43rd IEEE Conf. Decision and Control* (*CDC*) (*IEEE Cat. No. 04CH37601*), Nassau, Bahamas, 2004, pp. 602–607.

[6] D. K. D. Villa, A. S. Brandão, and M. Sarcinelli-Filho, A survey on load transportation using multirotor UAVs, *J. Intell. Robot. Syst.*, vol. 98, no. 2, pp. 267–296, 2020.

[7] M. R. Khosravi and S. Samadi, Mobile multimedia computing in cyber-physical surveillance services through UAV-borne Video-SAR: A taxonomy of intelligent data processing for IoMT-enabled radar sensor networks, *Tsinghua Science and Technology*, vol. 27, no. 2, pp. 288–302, 2022.

[8] H. X. Pham, H. M. La, D. Feil-Seifer, and M. C. Deans, A distributed control framework of multiple unmanned aerial vehicles for dynamic wildfire tracking, *IEEE Trans. Syst. Man Cybern, Syst.*, vol. 50, no. 4, pp. 1537–1548, 2020.

[9] P. Cevik, I. Kocaman, A. S. Akgul, and B. Akca, The small and silent force multiplier: A swarm UAV: Electronic attack, *J. Intell. Robot. Syst.*, vol. 70, no. 1–4, pp. 595–608, 2013.

[10] A. Hocraffer and C. S. Nam, A meta-analysis of human-system interfaces in unmanned aerial vehicle (UAV) swarm management, *Appl. Ergon.*, vol. 58, pp. 66–80, 2017.

[11] C. Yinka-Banjo and O. Ajayi, Sky-farmers: Applications of unmanned aerial vehicles (UAV) in agriculture. *Auton. Veh.*, pp. 107–128, 2020.

[12] F. Outay, H. A. Mengash, and M. Adnan, Applications of unmanned aerial vehicle (UAV) in road safety, traffic and highway infrastructure management: Recent advances and challenges, *Transp. Res. Part A Policy Pract.*, vol. 141, pp. 116–129, 2020.

[13] T. Rakha and A. Gorodetsky, Review of Unmanned Aerial System (UAS) applications in the built environment: Towards automated building inspection procedures using drones, *Autom. Constr.*, vol. 93, pp. 252–264, 2018.

[14] T. S. N. Rachmawati and S. Kim, Unmanned aerial vehicles (UAV) integration with digital technologies toward construction 4.0: A systematic literature review, *Sustainability*, vol. 14, no. 9, p. 5708, 2022.

[15] T. Dierks and S. Jagannathan, Output feedback control of a quadrotor UAV using neural networks, *IEEE Trans. Neural Netw.*, vol. 21, no. 1, pp. 50–66, 2010.

[16] X. Li, J. Tan, A. Liu, P. Vijayakumar, N. Kumar, and M. Alazab, A novel UAV-enabled data collection scheme for intelligent transportation system through UAV speed control, *IEEE Trans. Intell. Transport. Syst.*, vol. 22, no. 4, pp. 2100–2110, 2021.

[17] Y. C. Paw and G. J. Balas, Development and application of an integrated framework for small UAV flight control development, *Mechatronics*, vol. 21, no. 5, pp. 789–802, 2011.

[18] T. T. Li, J. J. Xiong, and E. H. Zheng, Improved sliding mode control for robust trajectory tracking of a quadrotor UAV, in *Proc. 2020 7th Int. Conf. Information Science and Control Engineering* (*ICISCE*), Changsha, China, 2020, pp. 1908–1912.

[19] L. Cao, X. Hu, and Y. Guo, Robust adaptive backstepping control of UAV with lumped uncertainties, in *Proc. 2014 Int. Conf. Mechatronics and Control* (*ICMC*), Jinzhou, China, 2014, pp. 961–965.

[20] H. Li, Q. Liu, G. Feng, and X. Zhang, Leader-follower consensus of nonlinear time-delay multiagent systems: A time-varying gain approach, *Automatica*, vol. 126, p. 109444, 2021.

[21] I. Bayezit and B. Fidan, Distributed cohesive motion control of flight vehicle formations, *IEEE Trans. Ind. Electron.*, vol. 60, no. 12, pp. 5763–5772, 2013.

[22] S. Kim and Y. Kim, Optimum design of three-dimensional behavioural decentralized controller for UAV formation flight, *Eng. Optim.*, vol. 41, no. 3, pp. 199–224, 2009.

[23] J. Zhang, J. Yan, and P. Zhang, Multi-UAV formation

control based on a novel back-stepping approach, *IEEE Trans. Veh. Technol.*, vol. 69, no. 3, pp. 2437–2448, 2020.

[24] J. J. Slotine and S. S. Sastry, Tracking control of non-linear systems using sliding surfaces with application to robot manipulators, in *Proc. 1983 American Control Conf.*, San Francisco, CA, USA, 1983, pp. 132–135.

[25] G. Wu, N. Wang, and J. Ying, Research on distributed real-time formation tracking control of high-order multi-UAV system, *IEEE Access*, vol. 10, pp. 36286–36298, 2022.

[26] Y. Fei, P. Shi, and C. C. Lim, Robust and collision-free formation control of multiagent systems with limited information, *IEEE Trans. Neural Netw. Learning Syst.*, vol. 34, no. 8, pp. 4286–4295, 2023.

[27] Q. Shen, Y. Shi, R. Jia, and P. Shi, Design on type-2 fuzzy-based distributed supervisory control with backlash-like hysteresis, *IEEE Trans. Fuzzy Syst.*, vol. 29, no. 2, pp. 252–261, 2021.

[28] S. Li, C. K. Ahn, J. Guo, and Z. Xiang, Neural-network approximation-based adaptive periodic event-triggered output-feedback control of switched nonlinear systems, *IEEE Trans. Cybern.*, vol. 51, no. 8, pp. 4011–4020, 2021.

[29] B. Q. Li, M. Z. Zong, H. Che, and Z. L. Xiong, Robust control for unmanned aerial vehicles formation based on adaptive disturbance observer, in *Proc. 2021 33rd Chinese Control and Decision Conf.* (*CCDC*), Kunming, China, 2021, pp. 5243–5248.

[30] J. Wang, F. Bao, L. Han, X. Dong, Q. Li, and Z. Ren, Discrete sliding mode control for time-varying formation tracking of multi-UAV system with a dynamic leader, in *Proc. 2020 Chinese Automation Congress* (*CAC*), Shanghai, China, 2020, pp. 4950–4955.

[31] J. Zhang and J. Yan, A novel control approach for flight-stability of fixed-wing UAV formation with wind field, *IEEE Syst. J.*, vol. 15, no. 2, pp. 2098–2108, 2021.

[32] S. Islam, P. X. Liu, and A. El Saddik, Robust control of four-rotor unmanned aerial vehicle with disturbance uncertainty, *IEEE Trans. Ind. Electron.*, vol. 62, no. 3, pp. 1563–1571, 2015.

[33] H. Liu, T. Ma, F. L. Lewis, and Y. Wan, Robust formation control for multiple quadrotors with nonlinearities and disturbances, *IEEE Trans. Cybern.*, vol. 50, no. 4, pp. 1362–1371, 2020.

[34] W. Zhao, H. Liu, and F. L. Lewis, Robust formation control for cooperative underactuated quadrotors via reinforcement learning, *IEEE Trans. Neural Netw. Learning Syst.*, vol. 32, no. 10, pp. 4577–4587, 2021.

[35] Z. Lin, L. Wang, Z. Han, and M. Fu, Distributed formation control of multi-agent systems using complex Laplacian, *IEEE Trans. Autom. Control*, vol. 59, no. 7, pp. 1765–1777, 2014.

[36] Z. Lin, L. Wang, Z. Han, and M. Fu, A graph Laplacian approach to coordinate-free formation stabilization for directed networks, *IEEE Trans. Autom. Control*, vol. 61, no. 5, pp. 1269–1280, 2016.

[37] K. Fathian, S. Safaoui, T. H. Summers, and N. R. Gans, Robust distributed planar formation control for higher order holonomic and nonholonomic agents, *IEEE Trans. Robot.*, vol. 37, no. 1, pp. 185–205, 2021.

[38] H. Liu, Y. Li, and Z. Wang, Optimal guaranteed cost control for multi-agent systems with actuator faults, in *Proc. 2018 IEEE Int. Conf. Systems, Man, and Cybernetics* (*SMC*), Miyazaki, Japan, 2018, pp. 2001–2006.

[39] J. Sun, S. Boyd, L. Xiao, and P. Diaconis, The fastest mixing Markov process on a graph and a connection to a maximum variance unfolding problem, *SIAM Rev.*, vol. 48, no. 4, pp. 681–699, 2006.

[40] L. Xiao and S. Boyd, Fast linear iterations for distributed averaging, *Syst. Control Lett.*, vol. 53, no. 1, pp. 65–78, 2004.

[41] S. Boyd, Convex optimization of graph Laplacian eigenvalues, in *Proc. of the International Congress of Mathematicians*, Madrid, Spain, 2006, pp. 1311–1319.

[42] H. K. Khalil, *Nonlinear Control*. New York, NY, USA: Pearson Education Limited, 2015.

[43] P. C. Lusk, X. Cai, S. Wadhwania, A. Paris, K. Fathian, and J. P. How, A distributed pipeline for scalable, deconflicted formation flying, *IEEE Robot. Autom. Lett.*, vol. 5, no. 4, pp. 5213–5220, 2020.

[44] K. Fathian, D. I. Rachinskii, M. W. Spong, T. H. Summers, and N. R. Gans, Distributed formation control via mixed barycentric coordinate and distance-based approach, in *Proc. 2019 American Control Conf.* (*ACC*), Philadelphia, PA, USA, 2019, pp. 51–58.

Peiyu Zhang received the MS degree in mathematics from Hebei University, Baoding, China, in 2020. She is currently pursuing the PhD degree at School of Transportation Science and Engineering, Beihang University, Beijing, China. Her main research interests include vehicle platoon control, intelligent transportation systems, and robust optimization.

Daxin Tian received the PhD degree in computer application technology from Jilin University, Changchun, China, in 2007. He is currently a professor at School of Transportation Science and Engineering, Beihang University, Beijing, China. His research is focused on intelligent transportation systems, autonomous connected vehicles, swarm intelligent, and mobile computing. He was awarded the National Science Fund for Distinguished Young Scholars and the Distinguished Young Investigator of China Frontiers of Engineering in 2018. He is also a sensor member of the IEEE and served as the Technical Program Committee member/Chair/Co-Chair for several international conferences including EAI 2018, ICTIS 2019, IEEE ICUS 2019, IEEE HMWC 2020, GRAPH-HOC 2020, etc.

Dezong Zhao received the BEng and MS degrees from Shandong University, Jinan, China, in 2003 and 2006, respectively, and the PhD degree from Tsinghua University, Beijing, China, in 2010, all in control science and engineering. He is currently a senior lecturer in autonomous systems at James Watl School of Engineering, University of Glasgow, UK. His research interests include connected and autonomous vehicles, machine learning, and control engineering. His work has been recognised by being awarded an EPSRC Innovation Fellowship and a Royal Society-Newton Advanced Fellowship in 2018 and 2020, respectively.

Kan Guo received the BS degree from Beijing University of Posts and Telecommunications, China, in 2015, and the PhD degree in control science and engineering from Beijing University of Technology, Beijing, China, in 2022. Now, he is a postdoctoral reresearcher supported by the Zhuoyue Program of Beihang University, China. His research interests include intelligent transportation system, graph neural network, and traffic forecasting.

Jianshan Zhou received the BSc, MSc, and PhD degrees in traffic information engineering and control from Beihang University, Beijing, China, in 2013, 2016, and 2020, respectively. He is currently an associate professor at School of Transportation Science and Engineering, Beihang University, China. From 2017 to 2018, he was a visiting research fellow at School of Informatics and Engineering, University of Sussex, Brighton, UK. He was a postdoctoral researcher supported by the Zhuoyue Program of Beihang University and the National Postdoctoral Program for Innovative Talents from 2020 to 2022. He is or was the Technical Program Session Chair with the IEEE EDGE 2020, the IEEE ICUS 2022, the ICAUS 2022, the TPC member with the IEEE VTC2021-Fall track, and the Youth Editorial Board Member of *Unmanned Systems Technology*. He is the author or co-author of more than 30 international scientific publications. His research interests include the modeling and optimization of vehicular communication networks and air–ground cooperative networks, the analysis and control of connected autonomous vehicles, and intelligent transportation systems. He was the recipient of the First Prize in the Science and Technology Award from the China Intelligent Transportation Systems Association in 2017, the First Prize in the Innovation and Development Award from the China Association of Productivity Promotion Centers in 2020, the Second Prize in the Beijing Science and Technology Progress Award in 2022, the National Scholarships in 2017 and 2019, the Outstanding Top-Ten PhD Candidate Prize from Beihang University in 2018, the Outstanding China-SAE Doctoral Dissertation Award in 2020, and the Excellent Doctoral Dissertation Award from Beihang University in 2021.

Xuting Duan received the PhD degree in traffic information engineering and control from Beihang University, Beijing, China, in 2017. He is currently an assistant professor at School of Transportation Science and Engineering, Beihang University, China. His current research interests include vehicular ad hoc networks, cooperative vehicle infrastructure system, and internet of vehicles.